

RSC Advances



This is an *Accepted Manuscript*, which has been through the Royal Society of Chemistry peer review process and has been accepted for publication.

Accepted Manuscripts are published online shortly after acceptance, before technical editing, formatting and proof reading. Using this free service, authors can make their results available to the community, in citable form, before we publish the edited article. This *Accepted Manuscript* will be replaced by the edited, formatted and paginated article as soon as this is available.

You can find more information about *Accepted Manuscripts* in the [Information for Authors](#).

Please note that technical editing may introduce minor changes to the text and/or graphics, which may alter content. The journal's standard [Terms & Conditions](#) and the [Ethical guidelines](#) still apply. In no event shall the Royal Society of Chemistry be held responsible for any errors or omissions in this *Accepted Manuscript* or any consequences arising from the use of any information it contains.

**Enhanced in vivo tumour imaging by EDTA-Bis-GNGR functionalized core shell CdSe:
ZnS quantum dot: synergistic effect of active passive targeting**

Rashi Mathur^{a*}, Narmada Bag^a, Raunak Varshney^a, Firasat Hussain^b, Ankur Kaul^a, Neelam Kumari^a, Ramprakash Chauhan^c, Shivani Singh^a, Sweta Singh^a, Anil. K. Mishra^{a*}

^aDivision of Cyclotron and Radiopharmaceutical Sciences, Institute of Nuclear Medicine and Allied Science, Brig. S.K. Mazumdar Raod, Lucknow Road, Timarpur, Delhi – 110054

^bDepartment of Chemistry, Delhi University, New Delhi-110054, India

^cDepartment of Chemistry, SVGC Ghumarwin, Bilaspur, Himachal Pradesh-174021, India

**Corresponding Author: email: rashimathur07@gmail.com, akmishra63@gmail.com*

Abstract

It has been shown in one of our earlier studies that the homodimeric N₂S₂ system enhances the biocompatibility of semiconductor core shell CdSe: ZnS quantum dots by lowering their toxicity and optimizing the steric ligand packing density. In this study we functionalize the core shell quantum dots with the same homodimeric ligand and add two moieties of GNGR (Gly-Asn-Gly-Asp) peptide which contain the NGR motif known to target the CD13 receptors in tumour vasculature. The aim is to study the influence of active receptor based targeting by peptide and passive targeting by QD nanoconjugate on tumour imaging. The core shell CdSe:ZnS quantum dot were synthesised and conjugated with EDTA-Bis-GNGR ligand. The docking studies show high binding affinity of the synthesised quantum dot nanoconjugate to the CD13 receptor. The GNGR peptide was synthesised on solid phase using Fmoc chemistry, followed by its conjugation to EDTA-Bis-Cysteamine. The complete physicochemical characterisation of the ligand was done using ¹HNMR, ¹³CNMR and Mass. The comparative in vivo kinetics, biodistribution and tumour targeting by native GNGR, EDTA-Bis-GNGR and EDTA-Bis-GNGR-QD was studied in murines after radiolabelling with ^{99m}Tc. The changes observed in vivo on comparing the three are very interesting. A seven fold increase in tumour uptake is seen after nanoconjugation highlighting the synergistic effect of active passive targeting resulting in enhanced tumour imaging. This study thus opens up a new area where the nanoplatfoms can be designed to get the best of both targeting and potential theranostic applications.

Keywords: Active-Passive Targeting, Radiolabelling, Scintigraphy

1. Introduction

The use of quantum dots as optical probes in diagnostic, immunoassays and cell labelling has been extensively explored¹⁻³ but their translation into products of clinical relevance has been limited due to the inherent toxicity of the core shell which contains metals like cadmium⁴⁻⁶. The passivation of the core with a higher band gap inorganic material helps control the leaching out of the core⁷⁻⁸ however, the synthetic protocols use organic solvents which result in the formation of hydrophobic dots which cannot be used directly for biological applications. Hence the focus moved to the functionalization of these cadmium based core shell quantum dots with biocompatible ligands like antibodies, small molecules and peptides⁹⁻¹¹. These ligands helped in making the QD hydrophilic but resulted in reducing their core emissions due to steric hindrance. Therefore, the need arose to design biocompatible ligands which can not only optimize the steric packing density for effective targeting but also maintain the native core shell emissions.

Last decade saw an increased focus on development of molecules which can interact with the overexpressed receptors in neo-angiogenesis which is very important for tumour growth and proliferation. When panning through the peptide phage library it was found that the peptide with NGR motif showed specific targeting towards the CD13 receptors found in neoangiogenic tumour vasculature¹²⁻¹³ and also target the $\alpha_v\beta_3$ integrins¹⁴⁻¹⁶. Thus this tripeptide emerged as an important sequence for use in non-invasive imaging. It has been reported earlier in literature that the modification of these peptides in terms of their multimerisation, PEGylation and cyclization can improve their tumour targeting efficiency by enhancing the target to non-target ratio¹⁷⁻²².

Earlier studies show that the cyclic form of NGR show better binding to the CD 13 receptors as compared to the linear form. It was also observed that the targeting ability of the peptide to

desired site is greatly influenced by the two flanking moieties. This lead to several modifications in the structure of NGR²³⁻²⁸.

M. Oosterndrop et.al in 2008 reported the synthesis of cNGR labelled paramagnetic CdSe/ZnS quantum dots which was the first documentary proof for the *in vivo* application of cNGR as a target ligand for non-invasive imaging²⁹. In this study the streptavidin modified quantum dots were simultaneously conjugated with biotin-tagged cNGR and biotin-tagged Gd(III)-DTPA. Both MRI and two photon laser scanning microscopy (TPLSM) showed that the cNGR-pQD to be highly specific towards surface active angiogenic endothelial cells as compared to the normal cells and tissues both *in vitro* and *in vivo*. The dual modified contrast agent was highly selective and exhibited threefold higher MRI contrast in tumour than the non-conjugated QDs. Thus the ability of this peptide to target angiogenesis/ neovasculature has prompted us to modify the flanking moieties of the NGR motif to design a molecule which can be used for specific imaging utilizing the platform of quantum dots for enhanced uptake (nanotechnology based tumour vasculature targeting including active and passive targeting)¹⁶.

Here we have synthesised a linear tetrapeptide GNGR (Gly-Asn-Gly-Asp) and conjugated it to a homodimeric N₂S₂ ligand which is an EDTA-Bis-cysteamine. In one of our earlier study³⁰ we have shown that this bis ligand very effectively controls the *in vivo* toxicity caused due to the leaching out of the Cd⁺² ions by providing a chelating effect. In this study we have tried to evaluate that if a specific targeting moiety is attached to this ligand then will there be an *in vivo* synergistic effect of active passive targeting or will only one of the mechanism predominate. Each of the bis ligand has two targeting moieties i.e., GNGR peptide attached to it and many such conjugates are attached to the quantum dot surface. This type of system should be able to optimize the steric ligand packing while maintaining the emission of the core. The grafting of

this ligand on the surface of the core shell CdSe:ZnS quantum dots thus makes it a very interesting system to study as it has the potential to be also used as a theragnostic nanoplatform.

2. Experimental

2.1 Materials

Ethylenediamine tetraacetic (EDTA) anhydride, diisopropyl carbodimide (DIC), dimethoxytrityl chloride (DMT-Cl), triethylamine (Et₃N), dimethyl aminopyridine (DMAP), pyridine, cysteamine hydrochloride, trifluoroacetic acid (TFA), dichloromethane (DCM), acetonitrile (ACN), tetrahydro furan (THF), rink amide resin, Fmoc-Gly-OH, Fmoc-Arg(Pbf)-OH, Fmoc-Asn(Trt)-OH, dimethylformamide (DMF), piperidine, trifluoroacetic acid (TFA), acetonitrile (HPLC grade), dry diethyl ether, stannous chloride dehydrated (SnCl₂ .2H₂O) were used from Sigma-Aldrich. HOBt was obtained from Hi Media, INDIA. All the other reagents used were of analytical grade and as received. ^{99m}Tc was procured from Regional Centre for Radiopharmaceuticals (Northern Region), Board of Radiation and Isotope Technology (BRIT), Department of atomic energy, India were used. Abbreviations Fmoc: 9-fluorenylmethoxycarbonyl Boc: tert-Butyl carbamates Trt: triphenylmethyl, pbf: pentamethyldihydrobenzofuran 5-sulfonyl Arg: Arginine, Gly: Glycine, Asp: Asparagine

2.2 Methods

The synthesized materials are characterized by NMR measurements were carried out on a Bruker 400 MHz system. Mass spectroscopic analysis was performed using an Agilent 1100 System coupled with LC operation in ESI (Electro Spray Ionization) positive/ negative mode. UV-Vis scanning was done on a UV-Vis spectrophotometer from Molecular devices SpectraMax-M-II-E. Gamma ray spectrometer (type GRS23C) (Electronics Cooperation of India Pvt. Ltd.,) was used

for determining the amount of activity (γ -emitter) in the samples. Gamma scintillation camera (HAWKEYE) was used for imaging of animals. Analytical RP-HPLC was performed on Jasco HPLC system. A Phenomenex Jupiter 5 μ - C-18 300 Å (250 mm x 4.60mm, 5 μ) was used. The solvent system consisted of 0.1% TFA in H₂O (solvent A) and 0.1% TFA in CH₃CN: H₂O (90:10) (solvent B). Elution was achieved by applying a linear gradient from 100% A to 70% B in 35 min, at a flow rate of 1 ml/min. Peptide peaks were detected spectrophotometrically (223 nm).

2.3 Computational Methodology

The computational protocol involved the flexible docking assisted analysis of dynamic interactions of peptidic ligands with Aminopeptidase N (APN) also known as CD13. All the computational studies were performed with the molecular modelling software, Schrödinger, LLC, New York, NY, 2014 maestro 9.731.

The atomic coordinates of crystal structure of CD13, 4FYS has been retrieved from RCSB PDB and employed for docking analysis having resolution of 2.01Å³². The Human CD13, 4FYS, is dimeric zinc containing metallopeptidase and co-crystalized with peptidic substrate, angiotensin IV. The crystal structure was pre-processed by deleting the hetero-atoms, addition of hydrogen atoms and assignment of bond orders and correct atom types. Further, monomeric moiety was retained for optimization and refinement to obtained processed 3D structure of CD13 to employ in docking analysis. For docking analysis, the co-crystalized peptidic substrate, angiotensin IV and the linear and cyclic NGR peptide has been used as references with respect to our designed molecule EDTA-Bis-GNGR. On symmetry basis we have considered only a monomeric unit of EDTA-Bis-GNGR for computational studies. All these four molecules were minimized and optimized to obtain the lowest possible energy conformers in the force field OPLS2005 without

any constraints by using the Ligprep v2.9 module. These conformers were generated in protonation states at $\text{pH}=7.0 \pm 2.0$ with retained specified chirality's.

The optimized CD13 receptor, 4FYS and five low energy conformers of ligands were subjected to Flexible docking analysis by Induced Fit docking (IFD) analysis. IFD analysis was included to allow the flexibility to the ligands and receptor to visualize the binding pose and interactions dynamically at the active site of CD13, 4FYS. IFD studies involves the high-precision Glide XP scoring to predict the binding mode of the ligands. Docking post-processing was done including analysis of key interactions and binding affinity analysis.

2.4 Solid phase synthesis of (Gly-Asn-Gly-Arg) GNGR tetrapeptide

The Fmoc protected rink amide resin (200 mg) was swelled in 4 mL DCM for 60 min and drained. The Fmoc was then de-protected using 20% (v/v) solution of piperidine in DMF for 20 min. The first amino acid was coupled to the resin by using 4 (eq) of Fmoc-Arg (pbf)-OH relative to the resin capacity and 4.0 equivalents (eq) of HOBT and DIC each relative to amino acid and 2 mL of DMF, the mixture was shaken for 2 h. Then the mixture was washed with DMF (3×25mL), MeOH (3×25mL), and DCM (3×25mL) and dried in vacuum. The Fmoc group was de-protected and the corresponding N-de-protected peptide $-\text{NH}_2$ - Arg (pbf)-OH-CONH-Rink amide, a mixture of 4 (eq.) of Fmoc-Gly-OH relative to the resin and 4.0 equivalents of HOBT and DIC relative to amino acid and 2 mL of DMF was added. The resin solution was left for shaking for 2 h at room temperature. Further the mixture was dried and washed with DMF (3×25mL), MeOH (3×25mL), and DCM (3×25mL) respectively. Then in the next step Fmoc - Asn (Trt)-OH was coupled with the de-protected $-\text{NH}_2$ -Gly-NHCO-Arg (pbf)-CONH-Rink amide to form Fmoc -Asn (Trt)-CONH-Gly-NHCO-Arg (pbf)-CONH-Rink amide. Further washing of the resin and respective de-protection was carried out as described above. Finally,

Fmoc-Gly-OH was coupled with de-protected $\text{-NH}_2\text{-Asn (Trt)-CONH-Gly-NHCO-Arg (pbf)-CONH-Rink}$ amide in the similar way to get Fmoc-Gly-CONH-Asn (Trt)-CONH-Gly-NHCO-Arg (pbf)-CONH-Rink amide. The resin bounded peptide was finally de-protected with TFA cocktail (TFA/TIS/H₂O/EDA (9.5/0.2/0.2/0.1 v/v). Throughout the reaction the progress of amino acid coupling and de-protection of Fmoc group was monitored by the colour change of ninhydrin in the Kaiser test³³ and purified using HPLC.

2.5 Synthesis of Cysteamine DMT

This was followed by the synthesis of dimethoxytrityl protected cysteamine. 1.2 (eq) of DMT chloride (10mmol) was added to cysteamine hydrochloride (8.84mmol) in presence of catalyst DMAP (0.00084mmol) and Et₃N in neat pyridine as solvent in a 100 ml round bottom flask. The reaction mixture was stirred at room temperature for 72 h under inert atmosphere. The completion of the reaction was confirmed by TLC (DCM: MeOH 9:1). The solvent was evaporated to dryness. Then the solution was diluted with DCM and extracted with chilled water repeatedly to remove any trace amount of pyridine. The resultant reaction mixture in DCM was then dried with sodium sulphate, filtered and evaporated to dryness. The obtained compound was sticky and dark brown in colour with a yield of 80%. ¹H NMR (CDCl₃, 400 MHz): δ (ppm), 2.35 (t, 2H, $\text{-CH}_2\text{-S}$), 2.63 (t, 2H, $\text{-CH}_2\text{-NH}_2$), 3.79 (s, 6H, CH₃-O), 6.79-7.44 (m, 13H, phe nyl ring), ¹³C NMR (CDCl₃, 100 MHz): δ (ppm), 36.44 (-C-S), 41.14 (C-N), 55.24 (C-O), 65.62 (C-3Ph), 113.11, 126.53, 128.39, 129.42, 130.70, 137.33, 145.56, 158.06 (carbons of phenyl ring).

2.6 Synthesis of EDTA-Bis-cysteamine-DMT

The second step shows the conjugation of DMT protected cysteamine with EDTA. This was carried out by adding cysteamine-DMT (1.319mmol) to EDTA anhydride (2.638mmol) in

presence of Et₃N (384.39 μl) in ACN as solvent under reflux condition at 70 °C under inert atmosphere for 48 h. The completion of the reaction was checked by TLC in DCM: MeOH (9:1). After completion of the reaction the solvent was evaporated to dryness and the desired compound was extracted with DCM: H₂O. The organic layer was dried with sodium sulfate and then evaporated to complete dryness. The obtained brown coloured compound was then further precipitated with diethyl ether. The precipitate found was then repeatedly washed with diethyl ether and dried to give a light brown coloured powder with a yield of 75%. ¹H NMR (CDCl₃, 400 MHz): δ (ppm), 2.37(m, 4H, -CH₂-S), 3.02(m, 8H, -CH₂-NH, N-CH₂-CH₂-N), 3.79(m, 20H, -CH₂-COOH, -CH₂-CONH, CH₃-O), 6.64-7.35(m, CH₂ of phenyl ring). ¹³C NMR (CDCl₃, 100 MHz): δ (ppm), 31.69 (-C-S), 38.60(C-CONH), 45.59 (N-C-C-N), 56.49 (C-O), 65.60, 65.68, 65.97 (C-3Ph, -N-C-COOH, -N-C-CONH), 113.14, 126.62, 127.94, 130.67, 137.14, 145.37, 158.00 (C of phenyl ring) 168.79 (CO-NH), 170.00 (CO-OH). m/z (ESI) calculated for C₅₆H₆₂N₄O₁₀S₂ was 1014.39 (M)⁺ and found 1013. 6 (M-H⁺).

2.7 Solid phase synthesis of EDTA-Bis-GNGR ligand

The prepared Fmoc-Gly-CONH-Asn (Trt)-CONH-Gly-NHCO-Arg (pbf)- CONH-Rink amide was de-protected in 20% (v/v) solution of piperidine in DMF for 20 min. Then in the reaction mixture 4 equivalents of the synthesized DMT protected EDTA-Bis-Cysteamine relative to the resin capacity and 4 equivalents of HOBT and DIC relative to the ligand was added along with 2 ml of DMF and left for stirring for 2 h. The coupling was checked for completion with the help of Kaiser test. The reaction mixture was then dried and washed with DMF (3×25mL), MeOH (3×25mL), and DCM (3×25mL) respectively. De-protection and cleavage from the resin were carried out using a trifluoroacetic acid mixture (TFA/TIS/H₂O/ EDA (9.5/0.2/0.2/0.1 v/v/v/v/v)) for 2 h at room temperature. After de-protection, the solutions were concentrated and the

peptides were precipitated by cold diethyl ether. The white precipitate of the peptides was washed with cold diethyl ether and characterized by mass spectroscopy (ESI) m/z calculated for $C_{42}H_{74}N_{20}O_{16}S_2$ is 1178.50 and found to be 1175.9 corresponding to $[M-2H]^+$.

2.8 Synthesis of EDTA-Bis-GNGR-QD

After the synthesis by phase transfer extraction the EDTA-Bis-GNGR ligand was appended over the surface of red light emitting quantum dots. The reaction was taken in a solvent mixture of THF: H₂O (1:1). The quantum dots were precipitated from the pre-existing solvent CHCl₃, by the addition of methanol, dried and added to the reaction mixture containing the EDTA-Bis-GNGR ligand. The reaction was left for stirring overnight at room temperature under inert atmosphere. The surface passivation and completion of the reaction was confirmed by the change in colour of the reaction mixture. The reaction mixture was evaporated to dryness and repeatedly washed with chloroform to remove the uncoated quantum dots present. The final compound was dissolved in small quantity of water and lyophilized to obtain the solid compound.

2.9 Radiolabelling

The bio-distribution and pharmacokinetics of GNGR peptide, EDTA-Bis-GNGR ligand, and EDTA-Bis-GNGR-QD nano-conjugate was studied after radiolabelling with ^{99m}Tc using SPECT imaging. An aqueous solution of GNGR peptide (1mg/ml), EDTA-Bis-GNGR ligand (1mg/ml), and EDTA-Bis-GNGR-QD nano-conjugate (1mg/ml) was taken in a shielded vial and stannous chloride was added. Then the pH of the resulting solutions was adjusted to 6.5-7.0 with addition of 0.5M NaHCO₃. Further all the mixture was passed through 0.22 μm filters into three different sterile glass vials. Freshly eluted $^{99m}\text{TcO}_4^-$ (93.7MBq) was added to each vial and the resulting complex was incubated for 15 min at room temperature for optimum radiolabelling yield. For all

the complexes the radiolabelling efficiency was estimated chromatographically using ITLC-SG as the stationary phase and 100% acetone as the mobile phase. The absence of free and unbounded $\text{Na}^{99\text{m}}\text{TcO}_4^-$ was evident from the paper chromatography.

2.10 In vitro serum stability studies

The metabolic stability of the GNGR peptide, EDTA-Bis-GNGR ligand, and EDTA-Bis-GNGR-QD nano-conjugate was ascertained in vitro in freshly collected serum from healthy animals. The collected serum was prepared by allowing blood collected to clot for 1hr at 37°C in a humidified incubator maintained at 5% carbon dioxide and 95% air. The samples were then centrifuged and the serum was filtered through a 0.22 μm filter into sterile plastic culture tubes. 100 μL of $^{99\text{m}}\text{Tc}$ labelled formulations were incubated respectively in 900 μL of this serum (in duplicate) at 37°C and analysed to check for any dissociation of the complex by ITLC using silica gel strips and 0.9% NaCl aqueous solution (saline) as developing solvent. The change in labelling efficiency was monitored over a period of 24 hr.

Animal Handling and Preparation for in vivo Studies: All animal experiments and study protocols were approved by the Committee for the Purpose of Control and Supervision of Experiments on Animals (CPCSEA), Government of India, New Delhi. Animal handling and experimentation were carried out as per the guidelines of the Institutional Animal Ethics Committee. Male spargue-dawly (SD) rats of age 6-8 weeks and Balb/C mice are given food and water ad libitum and housed in a 12h/12 h light and dark cycle.

2.11 Blood Kinetics and Bio-Distribution

Blood clearance of ^{99m}Tc -labeled nano-conjugates was studied in healthy SD rats ($n = 3$) $100\mu\text{Ci}$ of the radiolabelled complex in saline was administered intravenously through the tail vein of the rats. Blood samples were collected using the retro orbital procedure. The Blood was collected from this area in anesthetized rats using a micro-hematocrit tube at different time intervals ranging from 5 min to 24 h. Persistence of activity in the circulation was calculated as percentage injected dose per whole blood, assuming a total blood volume as 7% of the body weight. The radioactivity of the precipitate and supernatant was measured using a well-type gamma spectrometer.

Tumour bearing Balb/c mice with EAT grafted tumour on the left forelimb were used. The mice were administered 3.7 MBq of ^{99m}Tc labelled GNGR peptide, EDTA-Bis-GNGR ligand, and EDTA-Bis-GNGR-QD nano-conjugate, respectively, through the tail vein (i.v.). At 1, 2, 4 and 24 h post injection, the animals ($n = 3$) for each compound were euthanized and blood was collected by cardiac puncture into pre-weighed tubes. The mice were then dissected and different organs (heart, lungs, liver, spleen, kidneys, stomach, intestine, muscle (normal and tumour) were removed, weighed and their radioactive counts was taken with the help of a gamma counter. Uptake of the radio labelled compound into each organ was measured per gram of the tissue/organ and expressed as percentage injected dose per gram organ weight. The radioactivity remaining in the tail (point of injection) was also measured and taken into account while calculating the radioactivity.

2.12 Scintigraphic studies

Scintigraphic studies were performed on a gamma camera. $100\mu\text{L}$ of the radiolabeled GNGR peptide, EDTA-Bis-GNGR ligand, and EDTA-Bis-GNGR-QD nanobioconjugate, respectively,

injected through tail vein of Balb/c mice. The tumour was inoculated in the left forelimb of the mice using the EAT cell line.

3. Results and Discussion

3.1 Flexible Docking Analysis for EDTA-Bis-GNGR with Aminopeptidase-N (CD13)

The human CD13 structure, 4FYS in presence of a peptidic substrate, angiotensin IV shows its binding with key interactions at substrate binding and catalytic site. Induced fit docking (IFD) studies of peptidic substrate, angiotensin IV, linear & cyclic NGR (c-NGR) peptide and the designed molecule EDTA-Bis-GNGR was performed with 4FYS. The binding pose and geometry of the ligands at the site were screened on the basis of Glide XP score and further docking post-processing properties were obtained. The Glide XP score for angiotensin IV, linear NGR, cNGR peptide and designed molecule EDTA-Bis-GNGR were found to be -11.389, -9.772, -11.527 and -9.953 respectively. The flexible docking resulted in comparable G-score of EDTA-Bis-GNGR to other reference molecules. Ala353 has been considered as the key interacting residue as it is able to interact with all the reference molecules via hydrogen bonding. Existence of similar interaction in designed molecule EDTA-Bis-GNGR justify its ability to identify the correct substrate binding site. Secondly the range of hydrogen bond distance for EDTA-Bis-GNGR with Ala353 is of 2.16 Å^o which is quite comparable with the bond distance of 2.67Å^o for angiotensin, 2.31Å^o for cNGR and 1.70Å^o for linear NGR. This range of hydrogen bonding validates the good receptor binding affinity of EDTA-Bis-GNGR.

The common interacting residues in case of co-crystalized ligand angiotensin and proposed ligand EDTA-Bis-GNGR are found to be Ala 353, Glu 380, Arg381, Thr384, His388, Glh418, Tyr419 and Arg 442 but apart from this EDTA-Bis-GNGR is also capable to interact with some additional residues like Gly352, Asn438 and Glu 696. These large number of contributions

should be able to result in good binding pose (**Fig. 1a and 1b**). Hence, overall the flexible docking results provide us an insight into the ability of interaction and recognition of EDTA-Bis-GNGR at substrate binding site with good receptor affinity towards CD13. Molecular docking therefore predicts that the conjugation of GNGR with EDTA- Bis-cysteamine shows a good potential for targeting upregulated CD13 in angiogenic blood vessels.

3.2 Synthesis of EDTA-Bis-GNGR ligand

It is difficult to introduce peptide directly to the EDTA-Bis-cysteamine ligand due to the interference of –SH group or EDTA-Bis-cysteamine-QD nano-conjugate due to the complexity of purification and characterization. Therefore, a different synthetic strategy was designed and executed. As per the scheme shown in (**Fig. 2**) first the solid phase synthesis of GNGR peptide was done on rink amide resin using Fmoc chemistry. The peptide is purified by HPLC and is characterized using HRMS (ESI-TOF). GNGR retention time was $R_t = 3.9$ min. The molecular mass of the pure GNGR were determined by TOF HRMS $m/z =$ found: 402.5496 [M], Calculated: 402.2 (**S1**)

The simultaneous synthesis of Cysteamine – dimethoxytrityl chloride (1, **Fig.3**) was confirmed by the presence of characteristic multiplets in the ^1H NMR in the range of 6.5 to 7.4 ppm corresponding to the protons of phenyl ring and the singlet at 3.9 ppm due to the protons of methoxy (O-CH₃) group (**S2**). The ESI mass spectrum also shows two peaks at 402.0 and 303.2 corresponding to the $[\text{M}+\text{Na}^+]$ and fragmented dimethoxytrityl cation respectively (**S3**), the carbonyl carbon (-C=O). peaks at 168.79 and 170.00 ppm in ^{13}C NMR spectrum (2, **Fig.3**) confirms the synthesis of the newly formed amide and acid groups respectively as shown in (**S4**). The final step of conjugation of peptide with the final structure of EDTA-Bis-GNGR ligand was done using solid phase synthesis (3, **Fig. 3**) and was confirmed by ESI mass spectrum with

molecular ion peak at 1175 due to $[M-2H^+]$ as shown in (S5). The synthesis of EDTA-Bis-GNGR-QD (4 Fig. 3) nanobioconjugate was carried out by phase transfer extraction of the hydrophobic quantum dots. The size of the quantum dot nanobioconjugate was evaluated by transmission electron microscopy and it has been found to be less than 20 nm as shown in (Fig. 4).

3.3 In vitro serum stability studies

All the synthesized compounds GNGR peptide, EDTA-Bis-GNGR ligand, and EDTA-Bis-GNGR-QD nano-conjugate, were labelled with ^{99m}Tc for studying the radiolabelling efficiency. All the labelling parameters such as pH, concentration of reducing agents (SnCl_2), temperature etc. were standardized to achieve the maximum labelling efficiency. The proteolytic degradation of the radiolabeled nanobioconjugate was determined in mice serum in vitro. Instant thin layer chromatography of the prepared serum showed that the ^{99m}Tc -GNGR, ^{99m}Tc -EDTA-Bis-GNGR, and ^{99m}Tc -EDTA-Bis-GNGR-QD nano-conjugate, remained sufficiently stable during incubation at 37°C with the serum. A maximum of 5-6% of radioactivity degraded after 24 h of incubation advocating a high in vitro stability of almost 94-95% of all the radiolabelled complexes for up to 24 h.

3.4 Blood kinetics studies

The blood kinetics data clearly differentiates the pharmacokinetics of the peptide, quantum dot conjugated and non-conjugated ligands as shown in (Fig. 5). Where the native ^{99m}Tc GNGR shows the presence of only 4% activity in blood circulation in the first 15 min post injection, nearly 16% and 20% activity was found for the ^{99m}Tc - EDTA-Bis-GNGR ligand and ^{99m}Tc - EDTA- Bis-GNGR-QD conjugate. The circulation time was longer in case of quantum dot

conjugated system which may be due to the reduced opsonisation which is dependent on the surface chemistry and can lead to the decrease in non-specific uptake in the RES system. As per the result the native GNGR peptide has a very high clearance from the blood to tissues and also shows a fast clearance from the body. We had seen a similar behaviour in our previous studies where the circulation of the conjugate increases after attaching the quantum dot to the EDTA-Bis-cysteamine.³⁰ Here also in contrast to the native GNGR peptide and EDTA-Bis-GNGR, EDTA- Bis-GNGR-QD nanobioconjugate show higher in vivo retention which is required for a good diagnostic imaging agent

3.5 Biodistribution and Scintigraphic Studies

The quantification of the tumour uptake of all the synthesized ^{99m}Tc radiolabelled compound was carried out by in vivo biodistribution and scintigraphy studies. In our previous work we had seen that EDTA-Bis-Cysteamine shows a charge dependent clearance from the body however, as soon as it is conjugated to the Quantum dots the pharmacokinetics changed thereby indicating the role of size in targeting.³⁰ Here we have seen that the radiolabelled peptide (^{99m}Tc-GNGR) shows maximum accumulation in liver 1, 4 and 24 h of post injection (29.46%ID/gm, 25.96%ID/gm, 7.47%ID/gm), followed by spleen (19.42%ID/gm, 14.085ID/gm, 2.14%ID/gm) respectively as shown in (**Fig. 6a**). As the activity was not present in kidney after several hours of post injection, the route of excretion was expected to be hepatobiliary. At the concentration of administration, the uptake of the radiolabelled peptide was not high in the tumour approximately 0.98 %ID/gm and hence the tumour-to-non-tumour ratio i.e., 2.71% ID/gm was also not significant. This can be attributed to the linear structure of the peptide and also due to the fact that the native peptide shows a very fast clearance from the body only 0.52% ID/gm present 4 h post injection. The higher uptake in liver and spleen also contributes in decreasing the tumour-to-

non-tumour contrast. This is also evident from the scintigraphic image of ^{99m}Tc radiolabelled GNGR peptide 4 h post injection shown in (**Fig. 7a**). However, ^{99m}Tc radiolabelled EDTA-Bis-GNGR ligand shows a different distribution pattern. Here the conjugate shows a comparatively lower uptake in liver 1, 4 and 24 h of post injection i.e., 14.25 %ID/gm, 15.91 %ID/gm, 8.69 %ID/gm and spleen i.e., 6.85 %ID/gm, 10.24 %ID/gm, 4.15 %ID/gm as shown in (**Fig. 6b**). However, an increased uptake was observed in the kidney, stomach and intestine indicating a partial renal clearance along with the hepatobiliary route. There is an expected increase in the tumour uptake just after 4 h post injection i.e. 4.02 %ID/gm which increases gradually over 24 h. This may be because the ^{99m}Tc -EDTA-Bis-GNGR ligand has a comparatively increased circulation time in blood stream as evident from the radioactivity present in blood after 4 h of post injection i.e. 3.08 %ID/gm. This might be giving ample time for the radiolabelled conjugate to reach the site of interest and of course the bivalent effect of Bis-GNGR also plays an important role in this higher uptake. Therefore, we can infer that here the increased accumulation at tumour site can be attributed basically to the active targeting of the Bis-GNGR ligand. Interestingly the tumour-to-muscle ratio increases from 1.81 %ID/gm to 4.00 %ID/gm from 4h to 24 h post injection. The increased uptake in tumour is clearly visible in the scintigraphic image shown in (**Fig. 7b**).

However, when the ^{99m}Tc -EDTA-Bis-GNGR is conjugated to CdSe/ZnS coreshell quantum dots, a very interesting and different biodistribution pattern is observed. There is a dramatic decrease in the uptake at 1, 4, and 24h post injection in the liver (i.e., 3.82 %ID/gm, 5.47 %ID/gm, and 0.50 % ID/gm) and spleen (i.e., 2.23%ID/gm, 7.11%ID/gm, and 1.12% ID/gm) respectively as shown in (**Fig. 6c**). This may be due to the fact that the kind of surface modification that has been done in this study might reduce the chance of opsonisation, a critical factor responsible for

the high non-specific accumulation of nanoparticles in MPS organs. This decrease significantly impacts the tumour-to-non-tumour contrast. Hence 4 h post injection the nanobioconjugates shows the highest uptake of 19.51%ID/gm activity in tumour (**Fig.7c**). The respective tumour to muscle ratio is also significantly high i.e. 7.85 %ID/gm 24h post injection. This can be explained by the increased circulation time of the quantum dot nanobioconjugate in blood stream than the other radiolabelled compounds. Activity in blood 1 hr post injection of ^{99m}Tc -EDTA-Bis-GNGR-QD is 4.91 %ID/gm, 1.49 %ID/gm for ^{99m}Tc -EDTA-Bis-GNGR ligand, and 0.49%ID/gm for ^{99m}Tc - GNGR nanobioconjugate respectively.

This increased uptake can be explained due to the fact that in addition to the bivalent effect of Bis-GNGR, there is large loading of EDTA- Bis-GNGR ligand over the CdSe/ZnS quantum dot surface which increases their specificity towards tumour site due to active targeting. As discussed in the introduction the multimerisation of the peptide is affective in improving the tumour homing affinity significantly. At the same time presence of quantum dot results in their passive targeting due the leaky vasculature of tumour microenvironment and the poor lymphatic drainage system through the EPR effect (enhanced permeation and retention). As a result, greater than 7-fold increase in tumour uptake of ^{99m}Tc -EDTA- Bis-GNGR-QD nanobioconjugate can be seen as compared to the native GNGR. This observation clearly highlights the impact of synergistic effect of active and passive targeting in tumour imaging.

4. Conclusions

To summarise we have seen that the molecular docking predicts that the conjugation of GNGR with EDTA-Bis-Cysteamine has shown the potential for targeting tumours with upregulated CD13 receptors. We have been able to synthesise a very effective system based on a nano platform for enhancing the tumour to non-tumour ratio. It is also evident that the quantum dots

can play a novel role in changing the biodistribution and the pharmacokinetics of the biological molecules. The steric ligand packing density is optimized by using the homodimeric system which in addition to the bivalent ligand limits the opsonisation process resulting in enhanced circulation time to make the targeting effective. The QD nanobioconjugates show a synergistic effect of active (due to specific biomolecules) and passive targeting (due to the size and charge of the QD) resulting in enhancing the accumulation of the imaging probes at the desired sites. The use of a chelating system like EDTA also endows this nanoconjugate with the possibility for therapy by replacing the ^{99m}Tc with $^{186,188}\text{Re}$ which shows similar chemistry and hence can be effective in targeted theranostics.

5. Acknowledgement

The authors would like to thank Director INMAS, for his constant support and encouragement in carrying out this work. We are also thankful to Delhi University, India for providing characterization facilities. One of the authors Narmada Bag is thankful to University Grants Commission, for the financial support.

6. References

1. B. Dubertret, P. Skourides, D. J. Norris, V. Noireaux V., A. H. Brivanlou, A. Libchaber, in vivo imaging of quantum dots encapsulated in phospholipids micelles, *Science*, 2981 (2002), 759-1762.
2. M. Bruchez, M. Moronne, P. Gin, S. Weiss, A. P. Alivisatos, semiconductor nanocrystals as fluorescent biological labels. *Cell*, 13 (1998), 2013-1016.
3. E. B. Voura, J. K. Jaiswal, H. Mattoussi, S. M. Simon, Tracking metastatic tumour cell extravasation with quantum dots nanocrystals and fluorescence emission-scanning microscopy, *Nat. Med.* 10 (2004), 993-998.
4. A. Nei, T. Xia, L. Maedler, N. Li, Toxic potential of materials at nano label. *Science*, 311(2006), 622-627.
5. N. Chen, Y. He, Y. Su, X. Li, Q. Huang, H. Wang, X. Zhang, R. Tai, C. Fan, The cytotoxicity of cadmium based quantum dots, *Biomaterials*, 31(2010), 1238-1244.
6. C. Kirchner, T. Liedl, S. Kudera, Cytotoxicity of colloidal CdSe and CdSe/ZnS quantum dots, *Nano. Lett.*, 5(2005), 331-338.
7. B.O. Dabbousi, J. Rodriguez-Viejo, F.V. Mikulec, J.R. Heine, H. Mattoussi, R. Ober, K.F. Jensen, M.G. Bawendi, (CdSe/ZnS) core shell quantum dots: synthesis and characterization of size series of highly luminescent nanocrystallites *J. Phys. Chem. B* 101 (1997) 9463–9475.

8. X. Peng, M.C. Schlamp, A.V. Kadavanich, A.P. Alivisatos, Epitaxial growth of highly luminescent CdSe/CdS core/shell nanocrystals with photostability and electronic accessibility. *J. Am. Chem. Soc.* 119(1997), 7019–7029.
9. W. R. Algar, A. J. Tavares, U. J. Krull, beyond levels: A review on the application of quantum dots as integrated components of assays, bioprobes, and biosensors utilizing optical transduction. *Anal. Chim. Acta*, 673(2010), 1-25.
10. X. Ji, J. Zheng, J. Xu, V.K. Rastogi, T.C. Chen, J.J. DeFrank, R.M. Leblanc, J. (CdSe/ZnS) quantum dots and organophosphorous hydrolase bioconjugate as biosensors for detection of paraoxon, *Phys.Chem. B* 109 (2005) 3793–3799.
11. E.R. Goldman, I.L. Medintz, J.L. Whitley, A. Hayhurst, A.R. Clapp, H.T. Uyeda, J.R. Deschamps, M.E. Lassman, H. Mattoussi, A hybrid quantum dot-antibody fragment fluorescence resonance energy transfer based TNT sensors. *J. Am. Chem. Soc.* 127 (2005), 6744–6751.
12. A. Curti, F. Curnis, W. Arap, R. Pasqualini, The neo-vasculature homing motif NGR- more than meets the eye. *Blood*, 112(2008), 2628-2635.
13. A. Corti, F. Curnis, Tumour vasculature targeting through NGR peptide based drug delivery systems. *Curr. Pharm. Biotechnol.* 12(2011), 1128-1234.
14. A. K. Fuzery, N. Mihala, P. Szabo, A. Perczel, R. Giavazzi, H. Suli-Vargha, Solution state conformation and degradation of cyclopeptides containing an NGR motif. *J. Pept.Sci.* 11(2005), 53-59.

15. F. Curnis, R. Linghini, L. Crippa, A. Cattaneo, E. Dondossola, A. Bachi, A. Corti Spontaneous formation of L-isoaspartate and gain of function in fibronectin. *J. Biol. Chem.* 2006,281,36466-36476.
16. F. Curnis, G. Arrigoni, A. Sachhi, Differential binding of drug containing the NGR motif to CD13 isoforms in tumour vessels, epithelia and myeloid cells. *Cancer Res*, 62(2002), 867-874.
17. Z. Liu, S. Liu, F. Wang, S. Liu, X. Chen, Non-invasive imaging of tumour integrin expression using 18F-labeled RGD dimer peptide with PEG4 linkers *Eur. J. Nucl. Med. Mol. Imaging*, 36(2009), 1296–1307.
18. I. Dijkgraaf, J. A. W. Kruijtzter, S. Liu, A. C. Soede, W. J. G. Oyen, F. H. M. Corstens, R. M. J. Liskamp, O. C. Boerman, Improved targeting of the $\alpha\beta3$ integrin by multimerisation of RGD peptides *Eur. J. Nucl. Med. Mol. Imaging* 34(2007), 267–27.
19. Z. Liu, G. Niu, J. Shi, S. Liu, F. Wang, S. Liu, X. Chen, ^{68}Ga -labeled cyclic RGD dimers with Gly3 and PEG4 linkers: promising agents for tumour integrin $\alpha\beta3$ PET imaging *Eur. J. Nucl. Med. Mol. Imaging*, 36 (2009) ,947–957.
20. Z. F. Su, G. Liu, S. Gupta, Z. Zhou, M. Rusckowski, D. Hnatowich, In vitro and in vivo evaluation of a technetium-99m-labeled cyclic RGD peptide as a specific marker of $\alpha\beta3$ integrin for tumour targeting. *BioconjugateChem*,13(2002), 561–70.
21. F. M. Veronese, Peptide and protein PEGylation: a review of problems and solutions. *Biomaterials*, 22 (2001), 405–17.

22. X. Chen, R. Park, A. H. Shahinian, J. R. Bading, P. S. Conti, Pharmacokinetics and tumour retention of 125I-labeled RGD peptide are improved by PEGylation. *Nucl. Med. and Biol.* 31 (2004) ,11–19.
23. W. Arap, R. Pasqualini, E. Ruoslahti, Cancer treatment by targeted drug delivery to tumour vasculature in a mouse model. *Science*, 279(1998),377-380.
24. G. Colombo, F. Curnis, G. M. S. De Mori, A. Gasparri, C. Longoni, A. Sacchi, R. Longhi, A. Corti, Structure-activity relationship of linear and cyclic peptides containing the NGR-tumour homing motif. *J. Biol. Chem.* 2002,277,47891-47897.
25. A. Von Wallbrunn, C. Waldeck, J. Holtke, M. Zuhlsdorf, R. Mesters, W. Heindel, C. Schafers, M. Bremer, In vivo optical imaging of CD13/APN expression in tumour xenograft. *J. Biomed. Opt.* 13(2008), 0111007.
26. A. H. Negusse, J. L. Miller, G. Ready, S. K. Drake, B. J. Wood, M. R. Dreher, Synthesis and in vitro evaluation of cyclic NGR peptide targeted thermally sensitive liposomes. *J. Control Release*, 143(2010), 265-273.
27. L. Adar, Y. Shamay, G. Journo, A. David, Proapoptotic peptide-polymer conjugates to induce mitochondrial dependent cell death. *Polym. Adv. Technol.* 22(2011),199-208.
28. A. Dirksen, S. Langereis, B. F. de Waal, M. H. van Genederen, E. W. Meijer, Q. G. de Lussanet, T. M. Hackeng, Design and synthesis of a bimodal target-specific contrast agent for angiogenesis. *Org. Lett.* 6(2004), 4857-4860.

29. M. Oosterndrop, K. Douma, T. M. Hackeng, A. Dirkesn, M. J. Post, M. A. Van Znadvroot, W.H. Backes, Quantitative molecular magnetic resonance imaging of tumour angiogenesis using cNGR labelled paramagnetics quantum dots. *Cancer Res*, 68(2008), 7676-7683.
30. N. Bag, R. Mathur, F. Hussain, N. Indracanti, S. Singh, S.Singh, R.P. Chauhan, K. Chuttani, A.K. Mishra, Synthesis and in vivo toxicity assessment of cdSe:ZnS quantum dots functionalized with EDTA-Bis-Cysteamine, *Toxicol. Res.*, 4, 2015, 1416- 1425.
31. Schrödinger, LLC, New York, NY, 2014; Protein prepwizard, Ligprep version 3.0, Glide version 6.2
32. A. H. M. Wong, D. Zhou, J. M. Rini, The X-ray Crystal Structure of Human Aminopeptidase N Reveals a Novel Dimer and the Basis for Peptide Processing,. *J. Biol. Chem.* 287 (2012), 36804-36813.
33. R. Varshney, P. P. Hazari, J. K. Uppal, S. Pal, R. Stromberg, M. Allard, A. K. Mishra, Solid phase synthesis, radiolabelling and biological evaluation of a ^{99m}Tc -labeled $\alpha\text{V}\beta 3$ tripeptide (RGD) conjugated to DOTA as a tumour imaging agent. *Cancer Biol. Ther.*, 11, 2011, 893-901

List Of Figures

Figure 1 a: Two dimensional..... showing the hydrogen bonds.

Figure 2 Solid phase synthetic scheme of (Gly-Asn-Gly-Arg) GNGR tetrapeptide

Figure 3: Synthetic scheme of EDTA-Bis-GNGR-QD nanobioconjugate

Figure 4 : TEM image of EDTA-Bis-GNGR-QD nanobioconjugate

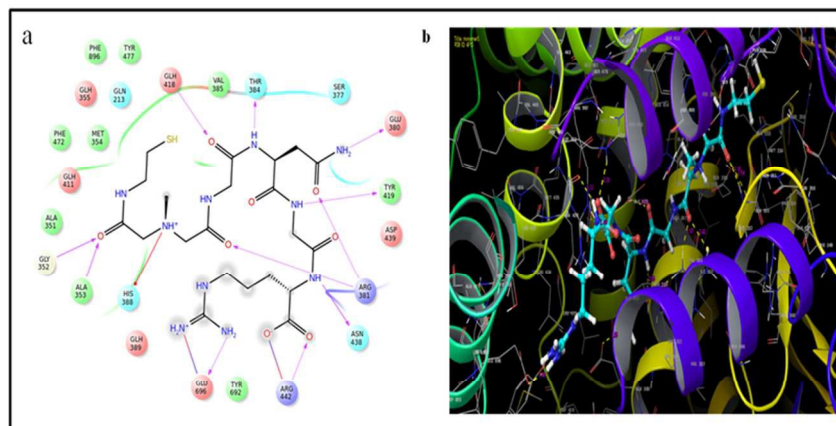
Figure 5: Blood kinetics profile of radiolabelled ^{99m}Tc -GNGR peptide, ^{99m}Tc -EDTA- Bis-GNGR ligand and ^{99m}Tc -EDTA- Bis-GNGR-QD

Figure 6 : Biodistribution pattern ^{99m}Tc labelled (a) GNGR (b) EDTA-Bis-GNGR (c) EDTA-Bis-GNGR-QD nanobioconjugate

Figure 7: Scintigraphic image of ^{99m}Tc labelled (a) GNGR, (b) EDTA-Bis-GNGR, (c) EDTA-Bis-GNGR-QD nanobioconjugate

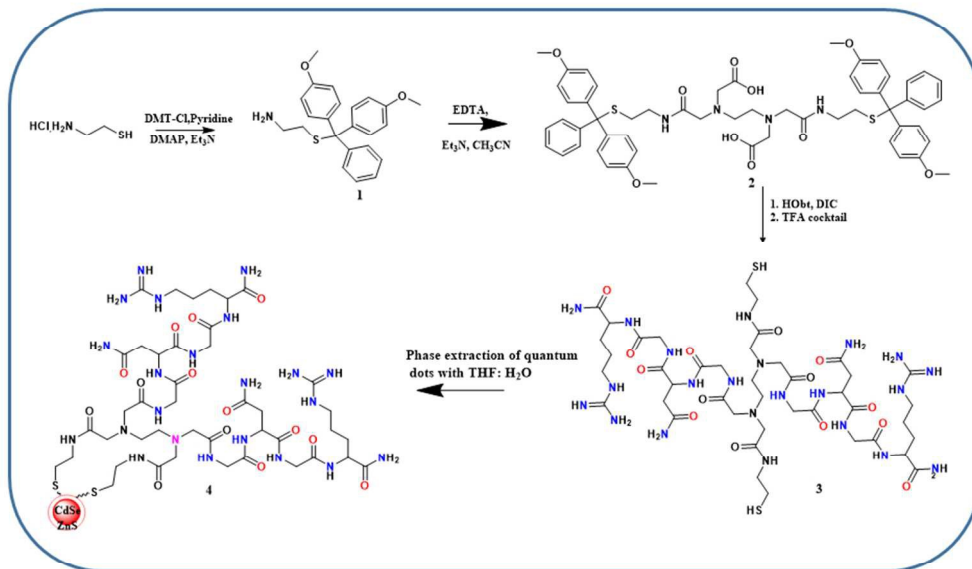
254x190mm (96 x 96 DPI)

Figure 1



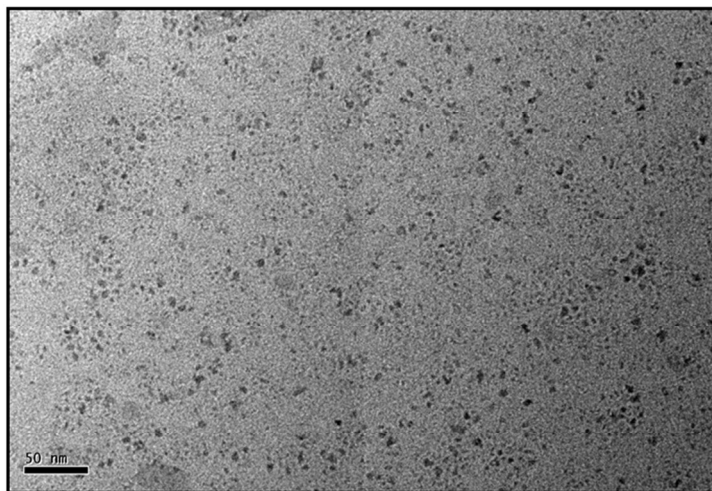
254x190mm (96 x 96 DPI)

Figure 3



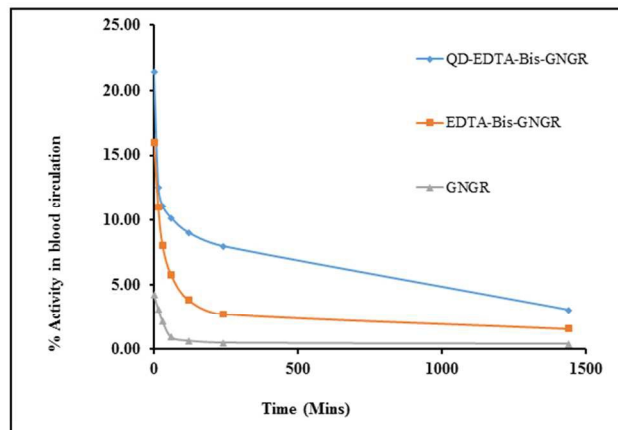
254x190mm (96 x 96 DPI)

Figure 4



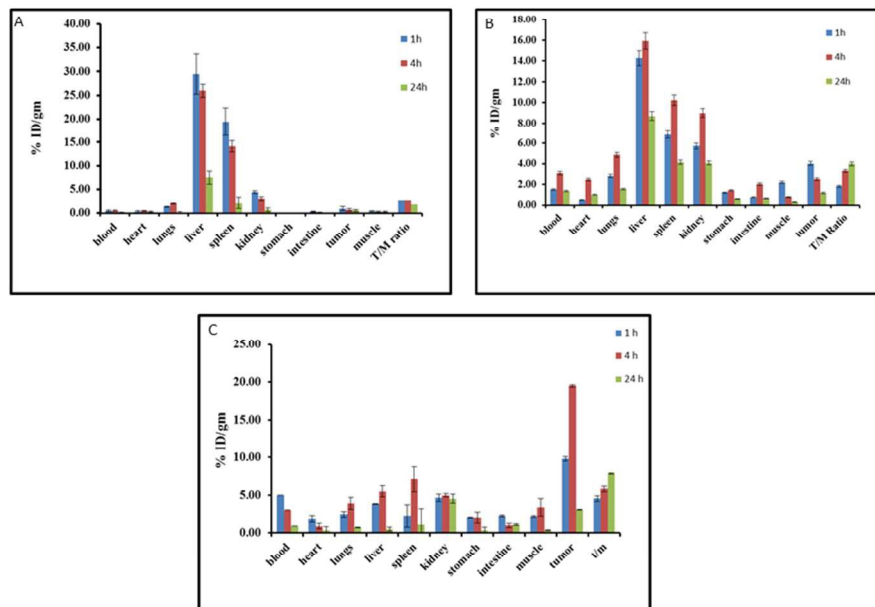
254x190mm (96 x 96 DPI)

Figure 5



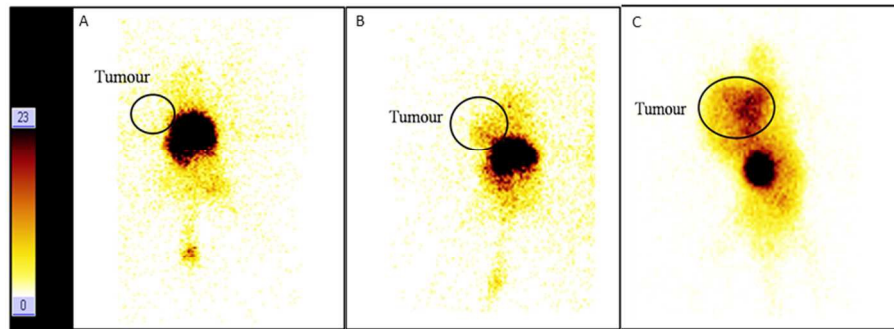
254x190mm (96 x 96 DPI)

Figure 6

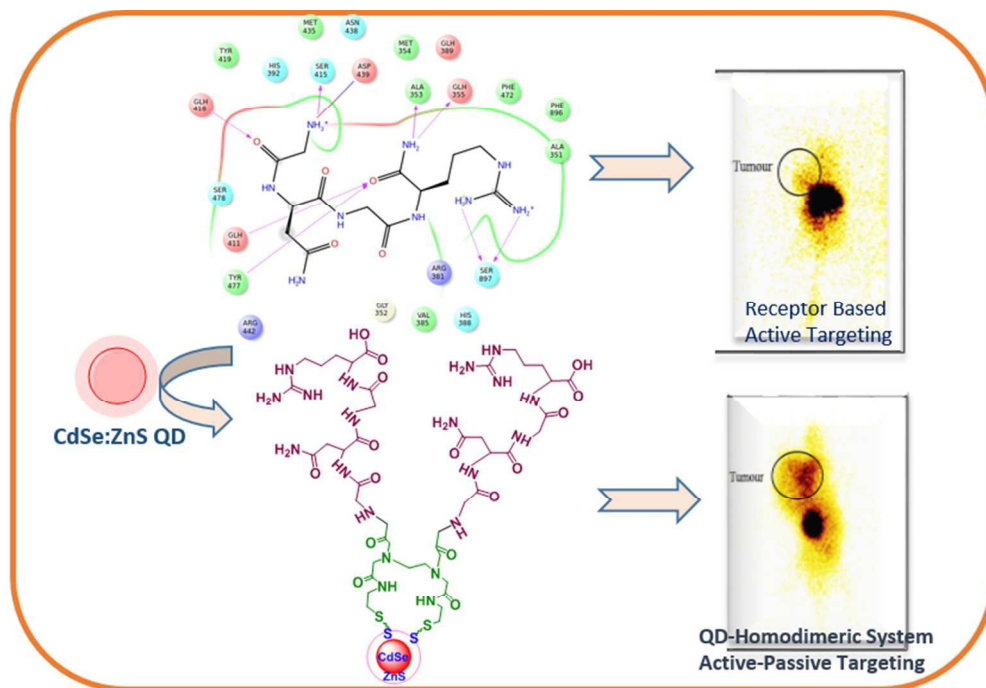


254x190mm (96 x 96 DPI)

Figure 7



254x190mm (96 x 96 DPI)



Use of QD-homodimeric system enhances tumour targeting due to the synergistic effect of active passive targeting

222x173mm (96 x 96 DPI)